scientific reports

Check for updates

OPEN

Impregnation of amine functionalized deep eutectic solvents in NH_2-MIL-53(Al) MOF for CO_2/N_2 separation

Narmin Noorani & Abbas Mehrdad✉

To improve the CO_2/N_2 separation performance of metal–organic frameworks (MOFs), amine functionalized deep eutectic solvents (DESs) (choline chloride/ethanolamine (DES1), choline chloride/ethanolamine/diethanolamine (DES2), and choline chloride/ethanolamine/methyldiethanolamine (DES3)) confined in the NH_2-MIL-53(Al). NH_2-MIL-53(Al) impregnated with DES was synthesized and characterized using N_2-sorption analysis and Fourier transform infrared (FTIR) spectroscopy. Morphology of the synthesized MOFs was investigated using scanning electron microscopy (SEM). Also, elemental analysis was determined by energy-dispersive X-ray spectroscopy (EDX). CO_2 adsorption isotherms of amine-functionalized DESs impregnated NH_2-MIL-53(Al) were measured at temperatures range of 288.15–308.15 K and pressures up to 5 bar. The results reveal that the impregnated MOF with functional group of amine DES improves separation performance NH_2-MIL-53(Al). CO_2 adsorption capacity of DES1/NH_2-MILS-53(Al) was twofold respect to of pristine NH_2-MIL-53(Al) at 5 bar and 298.15 K; which helps to guide the logical design of new mixtures for gas separation applications. Also, the heat of adsorption for the synthesized NH_2-MIL-53(Al) and DESs/NH_2-MIL-53(Al) were estimated. Most importantly, CO_2 chemisorption by NH_2 group in the sorbent structure has a significant effect on the adsorption mechanism.

One of the most significant challenges of world is climate change which its prevention and modification received widespread attention. Rapid economic growth and ongoing industrial development have resulted in an increase in the atmospheric carbon dioxide (CO_2) concentration from 270 ppm before the industrial revolution to 400 ppm now[1,2]. Hence, the emission of CO_2 has received widespread concern own to its ecosystem changes and environmental effects[3]. Rising global temperatures about 2 °C by the end of this century pose an urgent threat to the planet. The temperature increase of the earth is attributed to the greenhouse gases, of which CO_2 accounts for more than 70% of the total[4]. To overcome these troubles, the carbon capture and storage concept (CCS) was offered to control the CO_2 amount in the atmosphere[5]. As a key step in CCS, CO_2 is required to be captured from CO_2 emissions.

Technologies to separate CO_2/N_2 include membrane separation, molecular sieves, cryogenic separation, and absorption[6–9]. Current technologies employ aqueous amine solutions (monoethanolamine, diethanolamine and methyldiethanolamine), which adsorb CO_2 at ambient temperature in a thermally reversible manner[10]. Though this adsorption system has numerous advantages such as high reactivity, low cost and good adsorption capacity, it presents some serious disadvantages including solvent loss, emission of VOCs, corrosion and high energy required for the stripping of CO_2[11].

To overcome these disadvantages new technologies must be developed. Among the above-mentioned technologies, molecular sieves are of high interest due to the differences in the molecular size, diffusion, and gases affinity. Adsorption and separation of CO_2 using porous, solid adsorbents as an alternative for amine-based absorption/stripping processes has received much attention during the past decade. Metal–organic frameworks (MOFs), Zeolites, mesoporous silicas, and active carbons adsorbents have been tested for their CO_2 adsorption behavior[12,13].

Grafting of amines onto surfaces of porous materials to enhance adsorption of the acidic CO_2 molecule is another strategy that has been applied for silica-based sorbents and zeolites[14,15]. Arstad et al.[16] reported CO_2 adsorption isotherms on three new types of amine-functionalized MOFs. Adsorption capacities of up to 60 wt

Department of Physical Chemistry, Faculty of Chemistry, University of Tabriz, Tabriz, Iran. ✉email: a_mehrdad@tabrizu.ac.ir

% were obtained. Dautzenberg et al.[17] have studied aromatic amine-functionalized covalent organic frameworks (COFs) for CO_2/N_2 separation, The COF shows a high CO_2/N_2 IAST selectivity under flue gas conditions (273 K: 83 ± 11, 295 K: 47 ± 11). The interaction of the aromatic amine groups with CO_2 is based on physisorption, which is expected to make the regeneration of the material energy efficient. Ariyanto et al.[18] have studied DES-impregnated porous carbon which derived from the palm kernel shell for the separation of CO_2/CH_4. They indicated that separation performance increased in comparison to pristine porous carbon. Lin et al.[19] have investigated CO_2 capture in DES (choline chloride + ethylene glycol) confined into the graphene oxide (GO) with different HBA/HBD molar ratios by molecular dynamics simulation method and concluded that GO provides nanoconfined space for the DES. However, the isotherm data for DESs impregnated on MOFs for separation process is scarce. Metal–organic frameworks (MOFs) are a category of porous materials, which their structure is composed of metal ions networks or metal ion clusters and organic linkers connected through coordination bonds. MOFs own a high internal surface area, tunable multifunctional pores, adaptable porosity, and high thermal and chemical stabilities problems[20,21]. However, the capacity of adsorption of CO_2 in MOFs is quite low, and hence an enhancement is required. To improve the CO_2 adsorption capacity, the modification of MOFs using amines particularly monoethanolamine (MEA) can be performed because of availability, low cost, low viscosity, and high affinity to CO_2[22,23]. However volatile and corrosive nature are disadvantages of amines which led to an unsavory process. Thus, researchers have offered more efficient sorbents such as ionic liquids (ILs) and deep eutectic solvents (DESs) as potential alternatives for conventional amine solutions[24,25]. DESs due to unique properties including high solvation capacity, relatively low cost, higher biodegradability, and nontoxic make them environmentally and technologically superior alternatives to highly expensive ionic liquid[26]. In this research, three-component DESs were prepared by choline chloride:ethanolamine (1:7) (DES1), choline chloride: ethanolamine:diethanolamine (1:7:1) (DES2) and choline chloride:ethanolamine:methyldiethanolamine (1:7:1) (DES3). NH_2-MIL-53(Al) is composed of octahedral $AlO_4(OH)_2$ linked by a free-standing amine group[27]. In addition, NH_2-MIL-53(Al) has high pore volume, surface area, and thermal stability[28]. Also, the terephthalate ligands in NH_2-MIL-53(Al) can increase their compatibility with the DESs. In order to, DESs-impregnated NH_2-MIL-53(Al) was synthesized for CO_2 adsorption. The CO_2 adsorption in these DESs-impregnated NH_2-MIL-53(Al) was measured using quartz crystal microbalance (QCM). To study the potential of the material for separation purposes, adsorption isotherms were investigated. A novel hybrid model has been offered for correlating CO_2 isotherm. In addition, CO_2/N_2 selectivity was carried out to examine the practical efficacy of the prepared adsorbents.

Experimental

Materials. Aluminum nitrate nonahydrate ($Al(NO_3)_3{\cdot}9H_2O$) (> 99% purity), 2-amino terephthalic acid (NH_2-$H_2BDC \geq 99\%$), Choline chloride (> 99% purity), Ethanolamine (EA) (≥ 98% purity), diethanolamine (DEA)(≥ 98% purity), and methyldiethanolamine (MDE) (≥ 99% purity) were purchased from Sigma–Aldrich products. *N*,*N*-Dimethylformamide (DMF) (99% purity), Ethanol (> 99% purity) were supplied by Merck. CO_2 gas (> 99.9% purity) was used in gas absorption tests.

Synthesis of the DES. In this study, DES based on choline chloride as the HBA and ethanolamine, ethanolamine/diethanolamine, and ethanolamine/methyldiethanolamine as the HBD with special ratio were mixed to determine mole ratios under stirring at 360 K for about 2 h. Then obtained homogeneous solution had melting points below room temperature. The mole ratio of (HBA: HBD) and the melting point of DESs prepared are tabulated in Table 1 which resulted in good agreement with the literature[29].

Synthesis of NH_2-MIL-53(Al) and DES-confinement in NH_2-MIL-53(Al). Hydrothermal technique was used to synthesis NH_2-MIL-53(Al). for this purpose, 6.71 g of aluminum nitrate ($Al(NO_3)_3{\cdot}9H_2O$) was mixed with 3.74 g of 2-aminoterephthalic acid (NH_2-H_2BDC) and 50 mL of deionized water in a Teflon-lined autoclave at 423 K for 5 h. The obtained product was washed with acetone several times. The synthesized NH_2-MIL-53(Al) was treated at 423 K for about 48 h in DMF to eliminate the unreacted and trapped NH_2-H_2BDC in the pores[30]. DESs solution in ethanol with a ratio of 1:1 wt/vol was impregnated in NH_2-MIL-53(Al) using a vacuum impregnation method. To removal of ethanol, the obtained slurry was dried in oven at 378 K for 24 h.

Characterization of MOF. A FT-IR (Bruker, Tensor 27) spectrometer was used to recording the FT-IR spectra of NH_2-MIL-53(Al) and DESs/NH_2-MIL-53(Al). The morphology of synthesized MOF was investigated using providing FESEM images (EDX & Map & Line). X-ray diffraction (XRD) analysis (SHIMADZU, Labs XRD-6100) was conducted to determine particle size and crystalline structure. EDX spectra was recorded at 10 keV to distinguish the Al of the MOF. Nitrogen adsorption/desorption isotherms were recorded at 77 K (BELSORP MINI II instrument). The samples were degassed at 120 °C under vacuum condition for 10 h prior to

HBA	HBD	DES	Mole ratio	Melting point (K)
Choline chloride	Ethanolamine	DES1	(1:7)	275.2
Choline chloride	Ethanolamine/Diethanolamine	DES2	(1:7:1)	267.0
Choline chloride	Ethanolamine/Methyldiethanolamine	DES3	(1:7:1)	267.8

Table 1. Composition and molar ratio of investigated DESs.

the measurements. The BET surface area of the NH_2-MIL-53(Al) and DESs/NH_2-MIL-53(Al) were obtained by measuring the nitrogen adsorption at 77 K.

Gas adsorption apparatus. Gas adsorption measurements were done by QCM sensor. Detail of adsorption apparatus performance has been explained in the prior papers by authors[31–35]. The adsorption capacity, Q_e $\left(\mathrm{mg}_{CO_2} \cdot \mathrm{g}^{-1}_{\mathrm{DESs/MOF}}\right)$ was calculated as follows:

$$Q_e = \frac{\Delta F_S}{\Delta F_C} \times 1000 \tag{1}$$

where ΔF_C frequencies difference between the coated crystal with adsorbent and the uncoated crystal. ΔF_S is the difference between the frequencies adsorbent coated crystal under vacuum and after CO_2 adsorption.

Thermodynamic model. The CO_2 experimental isotherms achieved on NH_2-MIL-53(Al) in this study are correlated to the three-parameter Redlich–Peterson (R–P) model as follows[36]:

$$Q = Q_m \frac{cp}{1 + cp^n} \tag{2}$$

where Q related to the amount of adsorption per mass of adsorbent $\left(\mathrm{mg}_{CO_2} \cdot \mathrm{g}^{-1}_{\mathrm{DESs/MOF}}\right)$, p is gas pressure at equilibrium condition, n is the dimensionless adsorbent parameter and its value was considered as $n = 1$ in this study, also Q_m and c are parameters of model. Moreover, to correlate the experimental data of CO_2 solubility in DESs-impregnated on MOF a hybrid law of Henry and Redlich–Peterson (R–P) model are used as below:

$$Q = \frac{p}{H} + Q_m \frac{cp}{1 + cp^n} \tag{3}$$

where H is the CO_2 Henry's law constant.

The adsorption selectivity for CO_2/N_2 was calculated as follows:

$$S_{CO_2/N_2} = \frac{Q_{CO_2}}{Q_{N_2}}$$

where Q_{CO_2} and Q_{N_2} are adsorbed values of CO_2 and N_2, respectively.

Results and discussion

Characterization. *FT-IR spectra.* The FT-IR spectra of the NH_2-MIL-53(Al) and DES-impregnated on NH_2-MIL-53(Al) are illustrated in Fig. 1. As seen from Fig. 1 the symmetric and anti-symmetric N–H and O–H stretching vibrations of DESs are observed at 3300–3500 cm^{-1} and the single C-H stretching vibration is located at 2880–2950 cm^{-1}. C–N vibration is observed at 1086 cm^{-1}. Also, analysis of FT-IR peaks in Fig. 1d indicates the peak at 3400 cm^{-1} is related to the presence of NH_2 group MOF. The characteristic peaks at 1612 cm^{-1} and 1402 cm^{-1} are corresponding to the carboxylic acid which coordinated to Al[37]. Also, the peak at 1240 cm^{-1} is attributed to the C–N bending and the band observed at in the range of 965 cm^{-1} is attributed to aromatic C–H in-plane bending. Moreover, another band 629 cm^{-1} correspond with previous observations for MIL-53[38]. The characteristic peaks of both DESs and MOF are observed in DESs/NH_2-MIL-53(Al) (Fig. 1e–g) which is imply to success impregnation of DESs in MOF.

X-ray diffraction (XRD). The crystalline structure of NH_2-MIL-53(Al) and DES/NH_2-MIL-53(Al) were investigated using XRD spectra. XRD pattern of NH2-MIL-53(Al) and DES1/NH_2-MIL-53(Al) powder are illustrated in Fig. 2. From Fig. 2, it can be observed that the powder sample shows XRD peaks at 2θ values of 8.1°, 12.4°, 17.5°, 24.5° and 25.9° which confirmed the structure of NH2-MIL-53(Al)[39]. The characteristic peaks of NH2-MIL-53(Al) and DES1/NH_2-MIL-53(Al) are observed at the same angles which imply that crystalline structure of MOF remain unchanged during DES impregnation. However after impregnation the related peaks are broadened which attributed to the decreasing crystallinity degree.

EDX pattern. The distribution of different elements in NH_2-MIL-53(Al) was identified by EDX analysis. The pattern corresponding to the characteristic elements of NH_2-MIL-53(Al) is illustrated in Fig. 3. The results of the characteristic elements indicate that the mass fraction of C and N is 56.52% and 8.59%. The corresponding molar ratio of C to N is equal to 6.58, which is close to the molar ratio of C to N in the NH_2-H_2BDC structure. These results indicate the purity of the prepared NH_2-MIL-53 (Al) phase.

Scanning electron microscopy. Crystal morphology and size of the products were determined using SEM. SEM image of the NH_2-MIL-53(Al) is depicted in Fig. 4. As seen in the SEM image, the NH_2-MIL-53(Al) indicates a three-dimensional hexahedral structure with good regularity.

Textural properties of NH_2-MIL-53(Al). Nitrogen adsorption isotherms at 77 K were used to analyze the samples' textural characteristics, such as their specific surface area (A_{BET}), micropore volume (V_{MP}), and total pore volume (V_P). As depicted in Fig. 5, typical of microporous crystalline materials were obtained Type Ib isotherms[40]. In

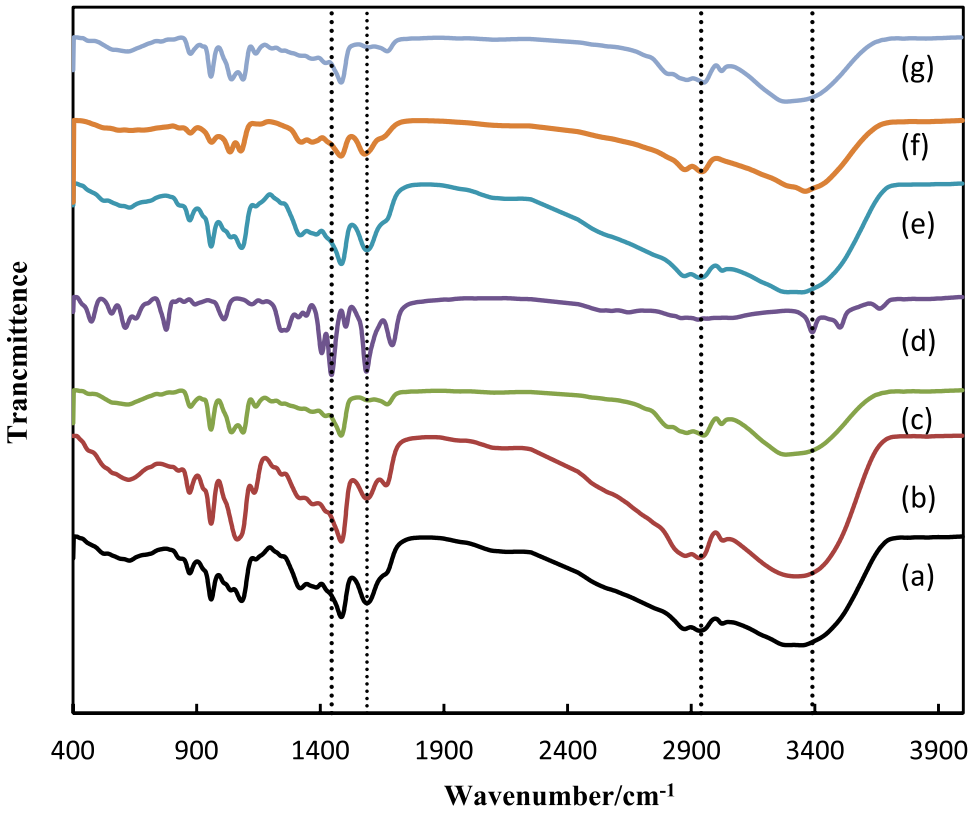

Figure 1. FT-IR spectra of the synthesized materials; (**a**) DES1; (**b**) DES2; (**c**) DES3; (**d**) NH_2-MIL-53(Al); (**e**) DES1/NH_2-MIL-53(Al), (**f**) DES2/NH_2-MIL-53(Al); (**g**) DES3/NH_2-MIL-53(Al).

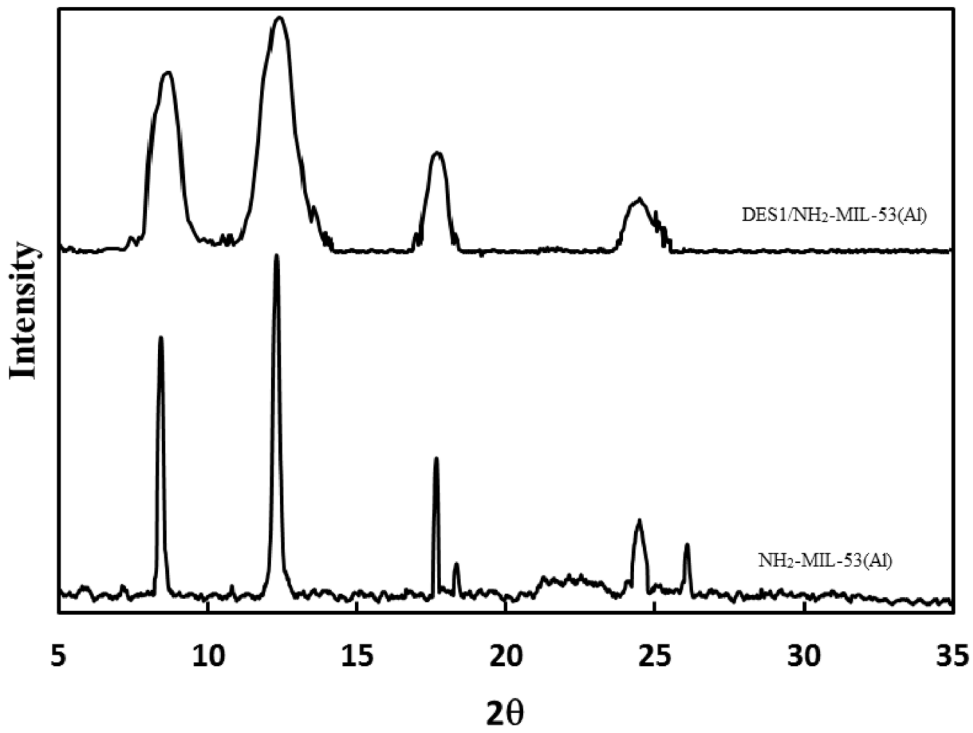

Figure 2. XRD pattern of NH2-MIL-53(Al) and DES1/NH_2-MIL-53(Al).

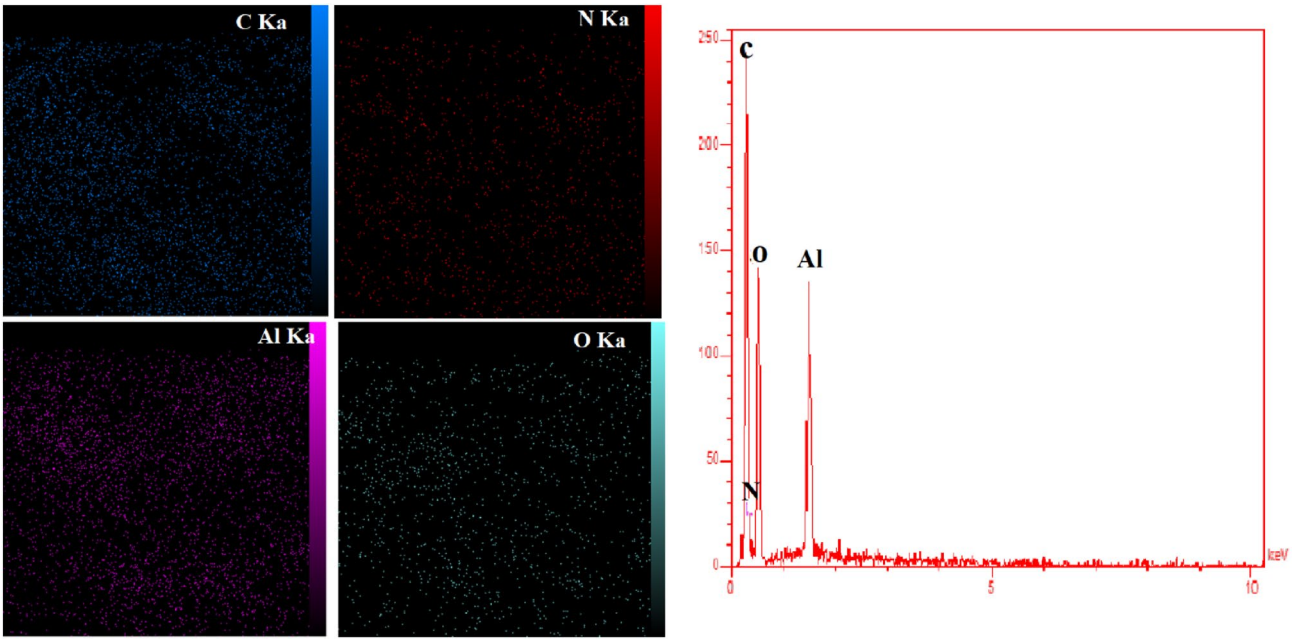

Figure 3. EDX patterns of the synthesized NH_2-MIL-53(Al).

other words, the N_2 isotherm of NH_2-MIL-53(Al) showed hysteresis behavior. The NH_2-MIL-53(Al) and DESs-impregnated NH_2-MIL-53(Al) samples displayed high volume adsorption at extremely low pressures, virtually achieving the maximum adsorption capacity. According to the isotherm of DES3-impregnated NH_2-MIL-53(Al), the sample had a low capacity for adsorption and a rise in adsorbed volume at relative pressures above 0.9, which are signs of macropore filling that may be caused by interstitial gaps. The textural properties of NH_2-MIL-53(Al) and DES/NH_2-MIL-53(Al) are reported in Table 2. The micropore volume and BET surface area of MOF is comparable with values reported in the literature[28,41]. The textural properties indicated that the impregnation procedure decreased the values of micropore volume, specific surface area and total pore volume relative to the original NH_2-MIL-53(Al) sample. Moreover, DES3/NH_2-MIL-53(Al), the higher the reduction in textural parameters and N_2 adsorbed volume at 77 K. This behavior reveals that DES molecules were incorporated in the pores of NH_2-MIL-53(Al) because of the impregnation process.

Adsorption isotherms. CO_2 and N_2 gas adsorption in NH_2-MIL-53(Al) and DESs-impregnated NH_2-MIL-53(Al) were measured at range temperature of 288.15–308.15 K and pressure of up to 5 bar. The CO_2 and N_2 gas adsorption data are tabulated in Tables 3 and 4. The experimental data of CO_2 and N_2 gas adsorption in NH_2-MIL-53(Al) and DESs-impregnated NH_2-MIL-53(Al) is correlated by the hybrid model. The parameters of the Redlich–Peterson (R–P) model q_m and c, and Henry's constant (H), for CO_2 and N_2 on the synthesized NH_2-MIL-53(Al) and DESs/NH_2-MIL-53(Al) are reported in Tables 5 and 6, respectively. The absolute average relative deviation is lower than 0.02, which implies to suitable capability of the proposed model. The calculated data indicate that the amount of CO_2 adsorbed was more than the amount of N_2 adsorbed. According to the data, the DESs-impregnated NH_2-MIL-53(Al) exhibit stronger adsorption and increases the CO_2 adsorption capacity. NH_2-MIL-53(Al) has a CO_2 adsorption capacity of 28.87 $mg_{CO_2} \cdot g^{-1}_{NH_2\text{ - MIL - 53}}$, while DESs-impregnated NH_2-MIL-53(Al), DES1/NH_2-MIL-53(Al), DES2/NH_2-MIL-53(Al), and DES3/NH_2-MIL-53(Al) have adsorption capacities of 62.68, 39.66, and 31.84 $mg_{CO_2} \cdot g^{-1}_{DES/NH_2\text{ - MIL - 53}}$, respectively at temperature of 298.15 K and pressure 5 bar. The isotherm curves of CO_2 and N_2 gas adsorption of the studied systems at different temperatures and pressures are illustrated in Fig. 6. In NH_2-MIL-53(Al) main interaction between CO_2 and MOF arises from carboxylate oxygen atoms and $-NH_2$ group in MOF, can increase preferential interactions between the frameworks and CO_2. In the MOF impregnated with DESs, gas adsorption arises from two factor; first factor is DESs which confinement in pores and second factor is DESs which immobilized in the surface of pores. The schematic interaction of DES with NH_2-MIL-53(Al) and CO_2 are illustrated in Fig. 7. With impregnation of DES in MOF a monolayer of DES is immobilized on the surface of MOF pores via hydrogen bond interactions. However residual DES so far away from surface which could not forming hydrogen bond. Therefore except of monolayer, the residual of DES is confined in the pores of MOF. When most of the pore surface of support is occupied by the immobilized DESs, the CO_2 sorption capacity of nano-confined DESs is dominated by the immobilized DESs rather than solid adsorbent. In the NH_2-MIL-53(Al) impregnated with DESs, at low pressure gas adsorption take placed on the immobilized DESs on surface of NH_2-MIL-53(Al); whereas at high pressure gas adsorption take placed on the confinement DESs on pores of NH_2-MIL-53(Al). Moreover, the chemical reaction between CO_2 molecules and the amine group affects the CO_2 adsorption NH_2-MIL-53(Al). Improving the pore characteristics of NH_2-MIL-53(Al) with different active sites, among which the creation of carboxylate oxygen atoms and NH_2 functional group, can increase preferential interactions between the frameworks and CO_2. The comparison of adsorption isotherm in DESs-impregnated NH_2-MIL-53(Al) was illustrated in

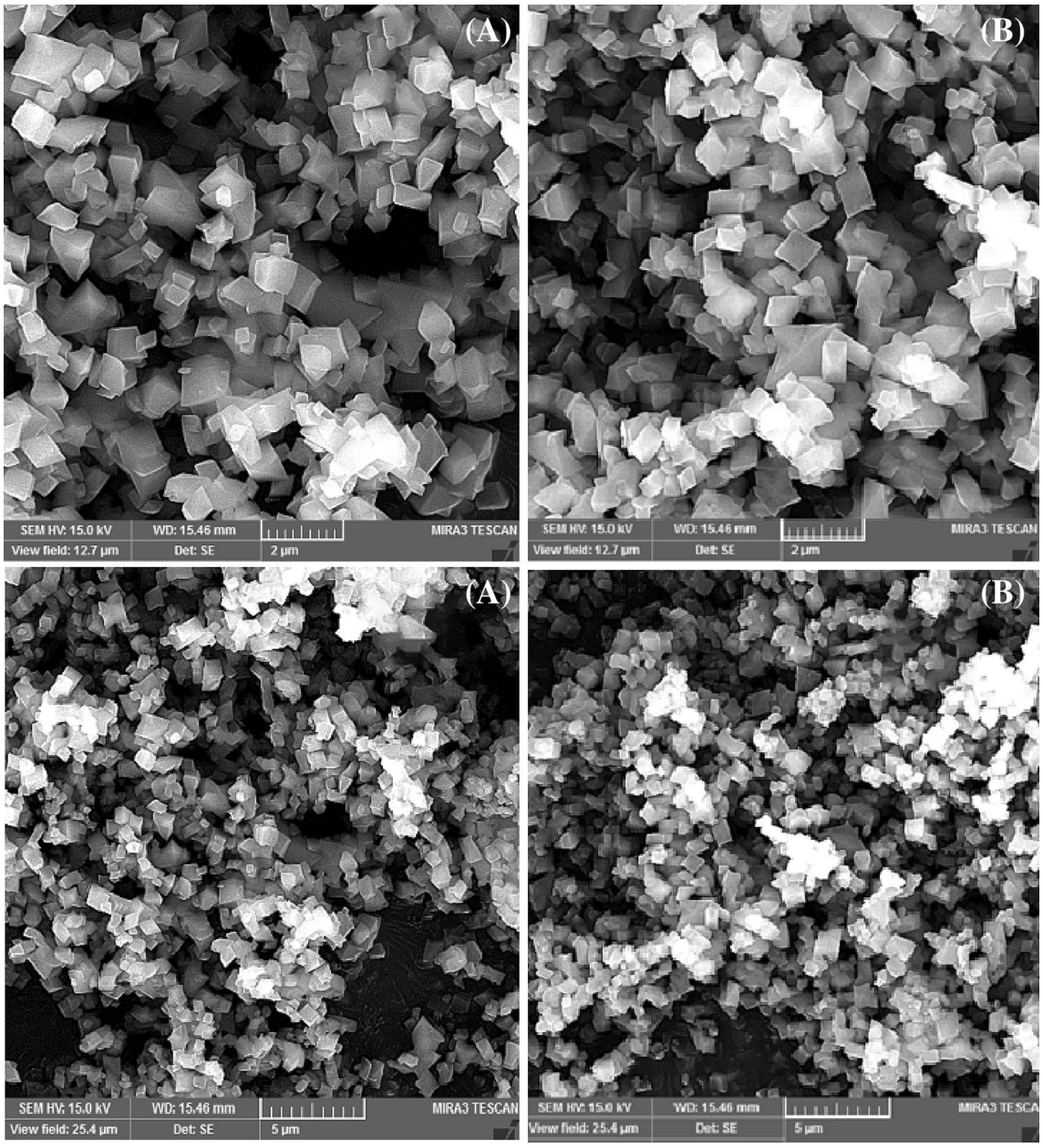

Figure 4. SEM images of (**A**) NH_2-MIL-53(Al) and (**B**) DES1/NH_2-MIL-53(Al).

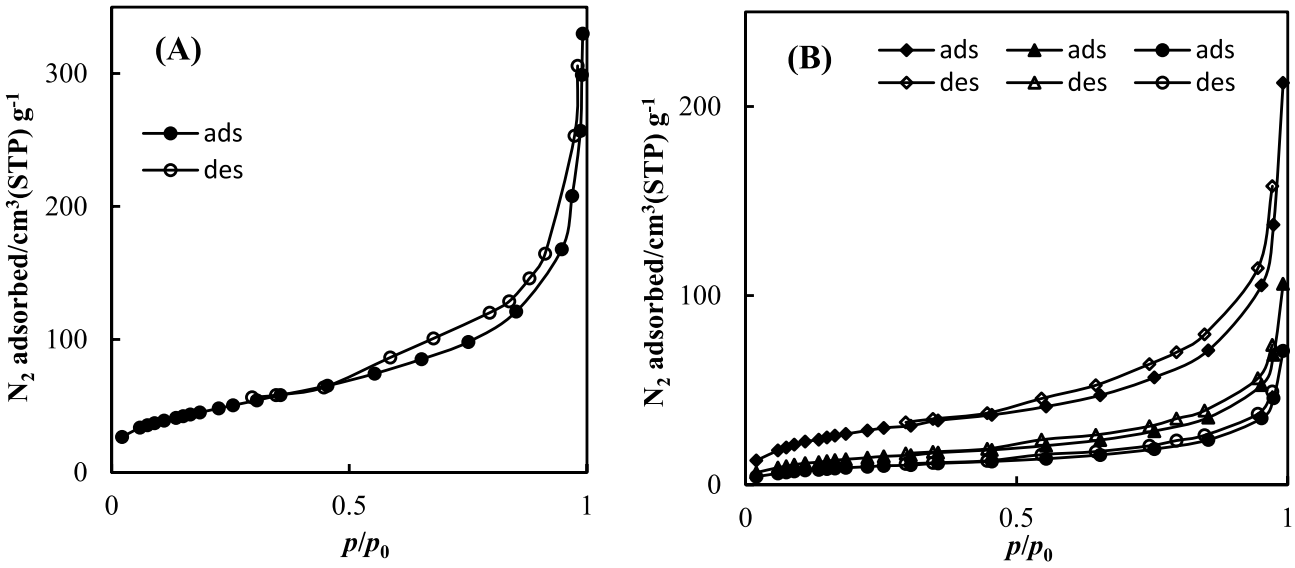

Figure 5. Nitrogen desorption–adsorption isotherms at 77 K: (**A**) in (●) NH_2-MIL-53(Al); and (**B**) (◆) DES1/NH_2-MIL-53(Al); (▲) DES2/NH_2-MIL-53(Al); (●) DES3/NH_2-MIL-53(Al).

DES /NH_2-MIL-53	A_{BET}/m^2 g^{-1}	V_P/cm^3 g^{-1}	V_{MP}/cm^3 g^{-1}
NH_2-MIL-53(Al)	635	0.32	0.27
DES1/NH_2-MIL-53(Al)	480	0.29	0.23
DES2/NH_2-MIL-53(Al)	435	0.25	0.21
DES3/NH_2-MIL-53(Al)	398	0.22	0.19

Table 2. Textural characteristics of the samples.

Fig. 8 at temperature of 298.15 K and pressure of up to 5 bar. The values of adsorption capacity follow the trend of: DES1/NH_2-MIL-53(Al) > DES3/NH_2-MIL-53(Al) > DES2/NH_2-MIL-53(Al). The highest CO_2 adsorption is corresponding to DES1/NH_2-MIL-53(Al) and the lowest adsorption is attributed to DES2/NH_2-MIL-53(Al), indeed, the addition of the secondary amine to DES1/NH_2-MIL-53(Al) reduced CO_2 adsorption. Reactivity of amines with CO_2 is in the order as Primary > Secondary > Tertiary. Hence, the addition of secondary amine decreased the absorption capacity of primary amine. Also, in DES3/NH_2-MIL-53(Al), when the tertiary amine is added to the DES1/NH_2-MIL-53(Al) adsorption capacity decreases however in compared to the DES2/NH_2-MIL-53(Al) the adsorption capacity increased due to the stronger intermolecular hydrogen bonds in DEA, consequently reaction between MDE and CO_2 is easier than reaction between DEA and CO_2 which leads to increase values of adsorption capacity. Overall, impregnation of MOF with DES1, DES2 and DES3 enhance the adsorption capacity about 130%, 14% and 52%, respectively. The similar results were reported in literatures. For example, Ariyanto et al.[18] have studied adsorption capacity of porous carbon which impregnated with three DESs (choline chloride:butanol, choline chloride:ethylene glycol and choline chloride:glycerol). They results reveals that the enhance adsorption capacity were 68%, 71% and 95%, respectively. The selectivity of CO_2/N_2 for NH_2-MIL-53(Al) and DESs/NH_2-MIL-53(Al) are shown in Fig. 9. The value of CO_2/N_2 selectivity decreases with increase in the pressure which is in good agreement with the literature[42,43]. DES1/NH_2–MIL–53(Al) displays batter selectivity with respect to the NH_2-MIL-53(Al).

$T = 288.15$ K		$T = 293.15$ K		$T = 298.15$ K		$T = 303.15$ K		$T = 308.15$ K	
p/bar	$Q_e/mg_{CO_2}.g^{-1}_{DES/MOF}$	p/bar	$Q_e/mg_{CO_2}.g^{-1}_{DES/MOF}$	p/bar	$Q_e/mg_{CO_2}.g^{-1}_{DES/MOF}$	p/bar	$Q_e/mg_{CO_2}.g^{-1}_{DES/MOF}$	p /bar	$Q_e/mg_{CO_2}.g^{-1}_{DES/MOF}$
NH_2-MIL-53(Al)									
0.422	7.3278	0.017	0.7	0.180	2.085	0.213	2.071	0.220	0.915
0.713	11.247	0.436	4.664	0.433	5.096	0.442	4.143	0.411	1.829
1.025	14.6844	0.615	7.229	0.671	7.413	0.646	5.984	0.590	2.515
1.500	19.121	0.824	9.562	0.859	8.802	0.834	7.135	0.807	3.430
2.000	23.273	1.090	11.894	1.070	10.656	0.995	8.285	0.978	4.116
2.500	27.088	1.500	16.558	1.500	13.899	1.500	11.277	1.500	6.174
3.000	29.971	2.000	19.522	2.000	17.142	2.000	14.039	2.000	8.004
3.500	32.482	2.500	22.754	2.500	19.921	2.500	16.110	2.500	9.833
4.000	34.66	3.000	25.318	3.000	21.774	3.000	17.491	3.000	11.434
4.500	36.503	3.500	27.317	3.500	23.628	3.500	19.333	3.500	13.035
5.000	37.643	4.000	29.282	4.000	25.481	4.000	21.483	4.000	14.864
		4.500	31.147	4.500	27.071	4.500	22.834	4.500	16.236
		5.000	32.013	5.000	28.897	5.000	24.915	5.000	17.837
DES1/NH_2-MIL-53(Al)									
0.250	8.689	0.017	2.182	0.278	2.915	0.218	4.414	0.477	7.549
0.436	14.482	0.272	8.000	0.532	11.662	0.412	9.458	0.682	9.872
0.685	20.999	0.480	13.818	0.663	14.577	0.610	11.98	0.979	12.776
0.915	26.068	0.668	18.182	1.006	20.408	0.860	15.763	1.500	16.841
1.500	37.654	0.945	23.273	1.500	27.697	1.096	18.916	2.000	20.325
2.000	47.067	2.000	41.455	2.000	32.799	1.500	23.96	2.500	23.229
2.500	55.033	2.500	47.273	2.500	40.087	2.000	28.373	3.000	25.552
3.000	62.274	3.000	52.364	3.000	43.003	2.500	32.156	3.500	29.036
3.500	70.239	3.500	57.455	3.500	47.705	3.000	35.939	4.000	31.359
4.000	76.756	4.000	63.273	4.000	52.478	3.500	38.462	4.500	34.482
4.500	83.997	4.500	67.636	4.500	56.309	4.000	41.614	5.000	37.885
5.000	89.790	5.000	71.773	5.000	58.682	4.500	44.136		
						5.000	46.028		
DES2/NH_2-MIL-53(Al)									
0.191	2.976	0.267	3.289	0.199	2.959	0.245	2.192	0.245	1.435
0.409	7.068	0.502	6.579	0.392	5.178	0.436	4.019	0.436	2.512
0.599	9.673	0.682	8.772	0.599	8.136	0.601	5.115	0.601	3.229
0.767	12.277	0.933	12.427	0.810	9.985	0.839	6.577	0.839	4.665
1.025	15.997	1.500	17.909	1.003	11.464	1.003	8.038	1.003	5.382
1.500	21.577	2.000	22.295	1.500	15.902	1.500	10.230	1.500	7.894
2.000	26.414	2.500	26.316	2.000	19.231	2.000	14.249	2.000	10.047
2.500	30.134	3.000	29.702	2.500	21.820	2.500	16.807	2.500	12.199
3.000	33.482	3.500	32.260	3.000	24.778	3.000	19.364	3.000	14.352
3.500	36.830	4.000	34.530	3.500	26.627	3.500	21.922	3.500	15.788
4.000	39.435	4.500	36.012	4.000	28.476	4.000	24.114	4.000	17.940
4.500	40.667	5.000	37.170	4.500	30.325	4.500	26.472	4.500	19.376
5.000	41.712			5.000	31.805	5.000	27.768	5.000	20.811
DES3/NH_2-MIL-53(Al)									
0.213	9.458	0.272	7.353	0.218	3.251	0.267	3.127	0.313	3.007
0.423	14.502	0.546	10.027	0.387	5.852	0.428	5.003	0.569	4.811
0.591	17.024	0.773	14.706	0.566	7.802	0.666	7.505	0.845	6.013
0.799	20.807	1.072	18.717	0.831	10.403	0.863	9.381	1.036	7.817
1.099	25.221	1.500	23.270	1.045	13.004	0.943	10.006	1.500	10.222
1.500	30.895	2.000	27.738	1.500	16.905	1.500	14.384	2.000	12.628
2.000	35.939	2.500	31.917	2.000	20.806	2.000	18.136	2.500	15.634
2.500	39.092	3.000	36.765	2.500	24.707	2.500	21.263	3.000	18.438
3.000	43.506	3.500	38.770	3.000	27.958	3.000	23.765	3.500	21.460
Continued									

$T = 288.15$ K		$T = 293.15$ K		$T = 298.15$ K		$T = 303.15$ K		$T = 308.15$ K	
p/bar	$Q_e/mg_{CO_2}.g^{-1}_{DES/MOF}$	p/bar	$Q_e/mg_{CO_2}.g^{-1}_{DES/MOF}$	p/bar	$Q_e/mg_{CO_2}.g^{-1}_{DES/MOF}$	p/bar	$Q_e/mg_{CO_2}.g^{-1}_{DES/MOF}$	p /bar	Q_e /$mg_{CO_2}.g^{-1}_{DES/MOF}$
3.500	47.919	4.000	42.112	3.500	31.209	3.500	26.941	4.000	24.452
4.000	49.811	4.500	46.123	4.000	34.460	4.000	29.393	4.500	26.860
4.500	52.963	5.000	48.797	4.500	38.061	4.500	31.895	5.000	29.661
5.000	55.485			5.000	41.262	5.000	34.396		

Table 3. CO_2 adsorption capacity $Q_e\left(mg_{CO_2} \cdot g^{-1}_{DES/NH_2\text{ - MIL - 53}}\right)$ of NH_2-MIL-53(Al), DES1/NH_2-MIL-53(Al), DES2/NH_2-MIL-53(Al), and DES3/NH_2-MIL-53(Al) at 288.15–308.15 K temperature range and pressures up to 5 bar. Standard uncertainties are u $(Q_e) = 0.010$, u$(T) = 0.05$ K, and u $(p) = 0.005$.

Enthalpy of adsorption. In order to evaluate the heat of adsorption, the adsorption experiments were carried out in the 288.15–308.15 K range temperature. The isotherms of the studied systems indicate that the adsorption isotherm are dependent to temperature while Mahdipoor et al.[44] indicate that the adsorption isotherm of MIL-101(Fe)–NH_2 is independent on temperature. Hence, the value of adsorption heat is assumed to equal the activation energy for primary alkanolamines. The molar enthalpy of absorption is a measure of interaction strength between the adsorbate molecule and the adsorbent surface identified isosteric heat of adsorption. The molar enthalpy of absorption is evaluated by calculated the gas adsorption at different temperatures[45,46]. Isosteric heat has calculated by differentiate an adsorption isotherm at a constant adsorbate loading which like as the Clausius–Clapeyron equation[47,48]:

$$\Delta H_S = R\left(\frac{\partial \ln p}{\partial\left(1/T\right)}\right)_q = -RT^2\left(\frac{\partial \ln p}{\partial T}\right)_q \tag{4}$$

where T and R, are temperature and universal gas constant, respectively. The effect of temperature on the CO_2 adsorption in DES1/NH_2-MIL-53(Al) sorbents is illustrated in Fig. 9. According to Fig. 10, the isosteric heat for NH_2-MIL-53(Al) and DESs/NH_2-MIL-53(Al) is obtained from plots ln(p) vs. 1/T. The value of isosteric heat for NH_2-MIL-53(Al) and DESs/NH_2-MIL-53(Al) are listed in Table 7. The calculated data for systems in this study indicate that the adsorption isotherm is dependent to temperature.

Regeneration efficiency of DES/NH_2-MIL-53(Al). Regeneration efficiency was used to evaluating adsorption/desorption performance of DES1/NH_2-MIL-53(Al) adsorbent. Five cycles of adsorption/desorption test in DES1/NH_2-MIL-53(Al) were tested to evaluation reuse capacity. The CO_2 adsorption capacity in five cycles of CO_2 adsorption/desorption test are illustrated in Fig. 11. In the adsorption/desorption test, CO_2 adsorption has tested at 298.15 K and 1 bar and desorption test was done in vacuum condition at 298.15 K for 90 min. The values of CO_2 adsorption are obtained as 20.408, 20.408, 20.407, 19.665 and 19.665 in five consecutive cycles of adsorption/desorption. The CO_2 adsorption capacity reduction in the DES1/NH_2-MIL-53(Al) compared to the fresh sample was estimated at about 4% after 5 cycles. This results confirms that the DESs/NH_2-MIL-53(Al) is stable and reusable under the practical condition of regeneration.

Conclusions

Deep eutectic solvents contain choline chloride in conjunction with different amines were impregnated in amino functionalized NH_2-MIL-53(Al) to improve the separation of CO_2/N_2. FTIR, SEM, EDX, and N_2-sorption analysis confirmed the impregnation of DES on porous MOF. The adsorption isotherms and separation tests of CO_2/N_2 revealed that DES1/NH_2-MIL-53(Al) exhibited a better performance. The obtained results indicate that in addition to physical adsorption of CO_2 by DES/NH_2-MIL-53(Al), CO_2 chemisorption by NH_2 functional group in the sorbent structure has also a notable effect on the adsorption mechanism. The DES1/NH_2-MIL-53(Al), can be employed repeatedly without losing separation performance and could increase the CO_2 uptake capacity twofold which introduce a novel category of highly porous adsorbents for the efficient adsorption of different compounds.

$T = 288.15$ K		$T = 293.15$ K		$T = 298.15$ K		$T = 303.15$ K		$T = 308.15$ K	
p/bar	Q_e/mg$_{CO_2}$·g$^{-1}_{DES/MOF}$	p/bar	Q_e/mg$_{CO_2}$·g$^{-1}_{DES/MOF}$	p/bar	Q_e/mg$_{CO_2}$·g$^{-1}_{DES/MOF}$	p/bar	Q_e/mg$_{CO_2}$·g$^{-1}_{DES/MOF}$	p/bar	Q_e mg$_{CO_2}$ · g$^{-1}_{DES/MOF}$
NH_2-MIL-53(Al)									
0.302	1.172	0.376	1.399	0.285	1.158	0.376	0.921	0.275	0.915
0.656	2.577	0.615	2.332	0.578	2.085	0.422	1.151	0.421	1.372
0.873	3.280	0.824	3.032	0.743	2.780	0.734	1.841	0.590	1.829
0.987	3.749	1.090	3.965	0.859	3.243	0.825	2.071	0.978	2.515
1.500	5.389	1.500	5.131	1.500	5.096	1.500	3.682	1.500	3.430
2.000	7.029	2.000	6.530	2.000	6.486	2.000	4.603	2.000	3.887
2.500	8.669	2.500	7.929	2.500	7.644	2.500	5.754	2.500	4.345
3.000	10.544	3.000	9.095	3.000	8.571	3.000	6.674	3.000	4.802
3.500	11.949	3.500	10.028	3.500	9.497	3.500	7.365	3.500	5.031
4.000	13.355	4.000	11.194	4.000	10.192	4.000	8.055	4.000	5.260
4.500	14.527	4.500	12.127	4.500	10.887	4.500	8.746	4.500	5.488
5.000	15.464	5.000	13.060	5.000	11.582	5.000	9.206	5.000	5.717
DES1/NH_2-MIL-53(Al)									
0.185	1.179	0.477	1.742	0.280	1.163	0.272	0.954	0.207	0.572
0.436	2.946	0.682	2.904	0.694	2.327	0.466	1.723	0.486	1.145
0.703	4.714	0.979	4.065	1.107	3.490	0.736	2.084	0.768	1.717
0.940	6.482	1.500	6.388	1.500	4.654	1.008	2.065	1.082	2.290
1.500	10.607	2.000	8.711	2.000	6.399	1.500	3.807	1.500	2.862
2.000	14.143	2.500	11.034	2.500	8.144	2.000	4.969	2.000	4.007
2.500	17.089	3.000	13.357	3.000	9.889	2.500	6.130	2.500	5.152
3.000	20.035	3.500	15.679	3.500	11.053	3.000	8.012	3.000	6.297
3.500	23.571	4.000	17.422	4.000	12.798	3.500	8.872	3.500	7.441
4.000	26.517	4.500	19.744	4.500	14.543	4.000	10.340	4.000	8.014
4.500	28.874	5.000	21.487	5.000	16.289	4.500	11.614	4.500	9.159
5.000	31.821					5.000	12.195	5.000	9.731
DES2/NH_2-MIL-53(Al)									
0.294	1.063	0.294	1.762	0.261	1.394	0.237	1.033	0.212	0.677
0.638	2.481	0.638	3.524	0.579	2.440	0.571	2.066	0.516	1.693
1.001	4.252	1.001	4.581	0.885	3.137	0.822	2.755	0.813	2.37
1.500	6.024	1.500	5.990	1.500	4.531	1.068	3.444	1.080	3.047
2.000	7.796	2.000	7.047	2.000	5.925	1.500	4.477	1.500	3.724
2.500	9.568	2.500	8.457	2.500	6.971	2.000	5.510	2.000	4.401
3.000	11.339	3.000	9.866	3.000	8.365	2.500	6.543	2.500	5.078
3.500	13.466	3.500	11.276	3.500	9.759	3.000	7.576	3.000	5.416
4.000	15.237	4.000	12.685	4.000	11.105	3.500	8.609	3.500	5.755
4.500	16.655	4.500	13.742	4.500	12.199	4.000	9.298	4.000	6.093
5.000	17.718	5.000	15.152	5.000	13.245	4.500	9.986	4.500	6.432
						5.000	10.675	5.000	6.77
DES3/NH_2-MIL-53(Al)									
0.166	0.910	0.180	0.930	0.270	1.017	0.213	0.913	0.226	0.903
0.414	1.820	0.632	2.791	0.444	1.848	0.527	1.826	0.535	1.805
0.591	2.730	0.943	3.721	0.845	2.773	0.717	2.740	0.904	2.708
0.788	3.640	1.500	5.581	1.274	4.621	1.001	2.740	1.500	3.610
1.017	4.550	2.000	7.442	1.500	5.545	1.500	4.566	2.000	4.513
1.500	7.279	2.500	9.302	2.000	7.394	2.000	5.479	2.500	5.415
2.000	9.099	3.000	11.163	2.500	8.318	2.500	6.393	3.000	6.318
2.500	10.919	3.500	13.023	3.000	10.166	3.000	8.219	3.500	7.220
3.000	13.649	4.000	14.884	3.500	12.015	3.500	9.132	4.000	8.123
3.500	15.469	4.500	16.744	4.000	13.863	4.000	10.046	4.500	9.025
4.000	17.288	5.000	18.605	4.500	14.787	4.500	10.959	5.000	9.928
4.500	19.108	0.180	0.930	5.000	15.712	5.000	11.872		
5.000	21.258								

Table 4. N_2 adsorption capacity Q_e ($mg_{CO_2}.g^{-1}_{DES/NH_2\ -\ MIL\ -\ 53}$) of NH_2-MIL-53(Al), DES1/NH_2-MIL-53(Al), DES2/NH_2-MIL-53(Al), and DES3/NH_2-MIL-53(Al) at 288.15–308.15 K temperature range and pressures up to 5 bar. Standard uncertainties are u (Q_e) = 0.010, u(T) = 0.05 K, and u (p) = 0.005.

DES/NH_2-MIL-53	T/K	H/bar	Q_m/$mg_{CO_2} \cdot g^{-1}_{AAILs/HKUST-1}$	c/bar^{-1}	R^2	[a]$AARD\%$
NH_2-MIL-53(Al)	288.15		62.521	0.306	0.9995	0.93
	293.15		60.028	0.238	0.9989	1.77
	298.15		49.646	0.261	0.9998	1.28
	303.15		40.199	0.263	0.9996	1.08
	308.15		95.485	0.046	0.9998	1.00
DES1/NH_2-MIL-53(Al)	288.15	0.086	42.430	0.691	0.9993	1.42
	293.15	0.102	30.660	0.939	0.9999	1.33
	298.15	0.125	28.830	0.711	0.9993	1.57
	303.15	0.159	19.950	0.855	0.9998	1.10
	308.15	0.168	8.320	0.679	0.9998	0.35
DES2/NH_2-MIL-53(Al)	288.15	0.439	48.480	0.390	0.9992	1.57
	293.15	0.379	39.670	0.364	0.9997	2.15
	298.15	0.338	23.535	0.567	0.9998	1.24
	303.15	0.274	15.857	0.364	0.9985	2.73
	308.15	0.268	3.515	0.980	0.9997	1.08
DES3/NH_2-MIL-53(Al)	288.15	0.155	27.840	0.661	0.9983	2.44
	293.15	0.159	21.310	0.742	0.9995	1.47
	298.15	0.156	10.210	0.856	0.9998	1.00
	303.15	0.177	7.890	0.503	0.9991	1.42
	308.15	0.179	1.510	0.433	0.9984	2.17

Table 5. Henry's law constant (H), Q_m and c are also parameters of the Redlich–Peterson isotherm model, the correlation coefficient (R^2) and absolute average relative deviation ($AARD$) for CO_2 adsorption on of NH_2-MIL-53(Al), DES1/NH_2-MIL-53(Al), DES2/NH_2-MIL-53(Al), and DES3/NH_2-MIL-53(Al) at different temperatures (T). Standard uncertainty is u(T) = 0.05 K. [a]$AARD\% = \frac{100}{n}\sum\left|\frac{Q^{cal}_{CO_2} - Q^{exp}_{CO_2}}{Q^{exp}_{CO_2}}\right|$.

DES/NH_2-MIL-53	T/K	H/bar	q_m/$mg_{CO_2} \cdot g^{-1}_{AAILs/HKUST-1}$	c/bar^{-1}	R^2	[a]$AARD\%$
NH_2-MIL-53(Al)	288.15		74.446	0.054	0.9990	1.36
	293.15		37.504	0.106	0.9998	0.76
	298.15		25.153	0.171	0.9996	1.28
	303.15		27.253	0.105	0.9991	2.29
	308.15		8.046	0.480	0.9994	1.14
DES1/NH_2-MIL-53(Al)	288.15	0.188	11.050	0.201	0.9987	2.08
	293.15	0.286	69.180	0.013	0.9994	1.17
	298.15	0.286	29.280	0.566	0.9988	1.93
	303.15	0.395	1.250	0.251	0.9990	1.84
	308.15	0.521	0.522	0.691	0.9993	1.91
DES2/NH_2-MIL-53(Al)	288.15	0.313	3.614	0.340	0.9992	0.65
	293.15	0.354	1.413	0.543	0.9986	1.52
	298.15	0.396	0.796	0.790	0.9988	1.57
	303.15	0.581	2.828	0.941	0.9974	1.80
	308.15	1.005	2.534	0.408	0.9988	0.89
DES3/NH_2-MIL-53(Al)	288.15	0.240	0.734	0.779	0.9994	1.18
	293.15	0.274	0.263	0.279	0.9993	1.25
	298.15	0.327	1.347	0.956	0.9985	2.36
	303.15	0.465	1.564	0.552	0.9990	1.41
	308.15	0.554	0.966	0.726	0.9991	1.37

Table 6. Henry's law constant (H), q_m and c are also parameters of the Redlich–Peterson isotherm model, the correlation coefficient (R^2) and absolute average relative deviation ($AARD$) for N_2 adsorption on of NH_2-MIL-53(Al), DES1/NH_2-MIL-53(Al), DES2/NH_2-MIL-53(Al), and DES3/NH_2-MIL-53(Al) at different temperatures (T). Standard uncertainty is u(T) = 0.05 K. [a]$AARD\% = \frac{100}{n}\sum\left|\frac{Q^{cal}_{CO_2} - Q^{exp}_{CO_2}}{Q^{exp}_{CO_2}}\right|$.

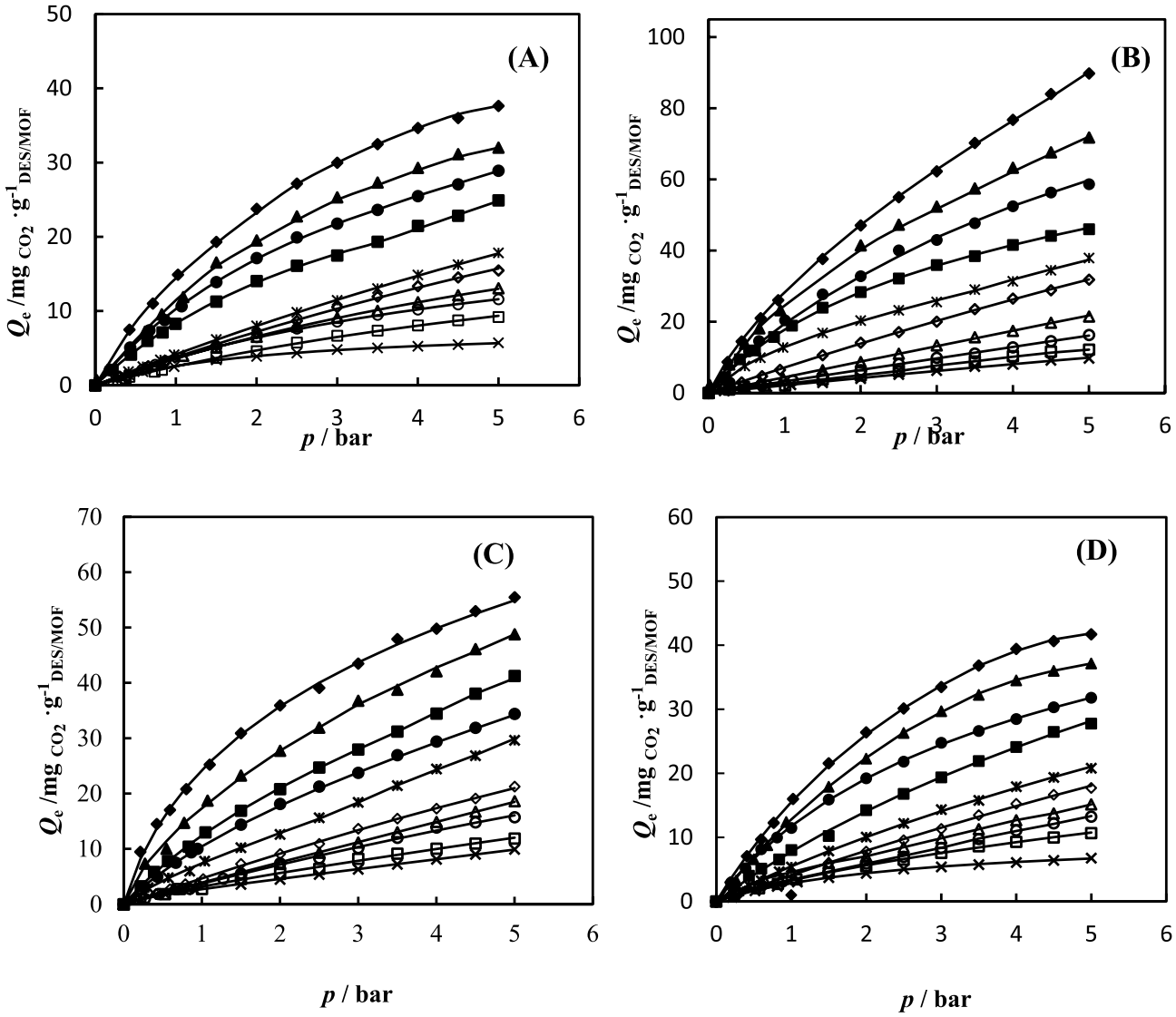

Figure 6. The CO_2 adsorption in (**A**) NH_2-MIL-53(Al); (**B**) DES1/NH_2-MIL-53(Al); (**C**) DES2/NH_2-MIL-53(Al); (**D**) DES3/NH_2-MIL-53(Al) at different temperatures (♦) 288.15 K; (▲) 293.15 K; (●) 298.15 K; (■) 303.15 K; (*) 308.15 K; the N_2 adsorption at different temperatures (◊) 288.15 K; (Δ) 293.15 K; (○) 298.15 K; (□) 303.15 K; (✖) 308.15 K; (–) fitting results by Eq. (3).

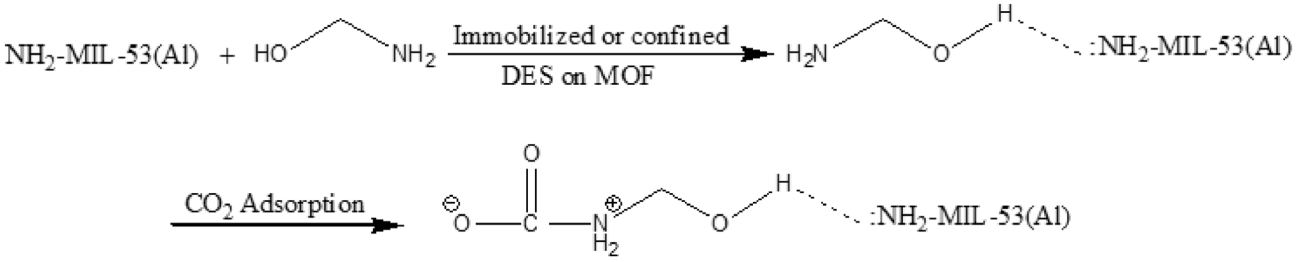

Figure 7. Schematic interaction of DES with MOF and CO_2.

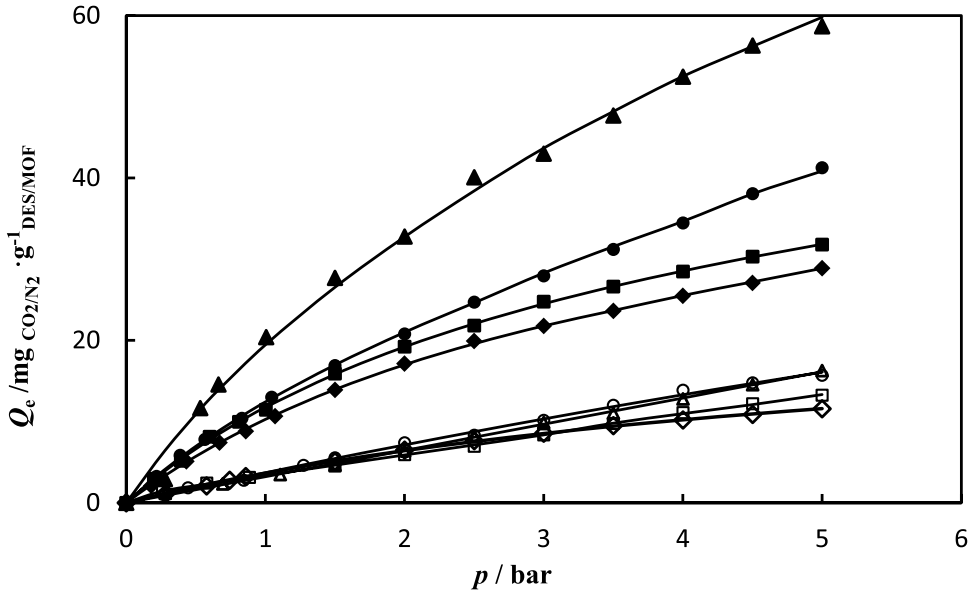

Figure 8. (**A**) The CO_2 adsorption in (◆) NH_2-MIL-53(Al); (▲) DES1/NH_2-MIL-53(Al); (●) DES2/NH_2-MIL-53(Al); (■) DES3/NH_2-MIL-53(Al); and N_2 adsorption in (◊) NH_2-MIL-53(Al); (Δ) DES1/NH_2-MIL-53(Al); (○) DES2/NH_2-MIL-53(Al); (□) DES3/NH_2-MIL-53(Al); at temperatures 298.15 K; (–) fitting results by Eq. (3).

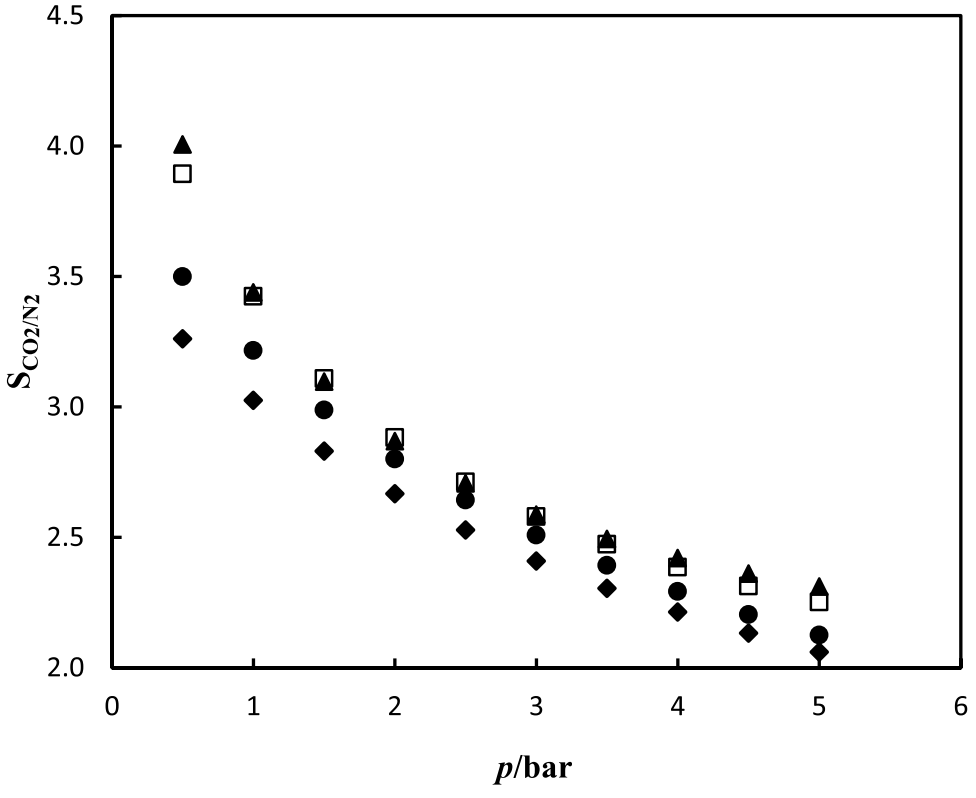

Figure 9. Selectivity of CO_2/N_2 versus pressure at temperature 293.15 K; (◆) NH_2-MIL-53(Al); (▲) DES1/NH_2-MIL-53(Al); (●) DES2/NH_2-MIL-53(Al); (□) DES3/NH_2-MIL-53(Al).

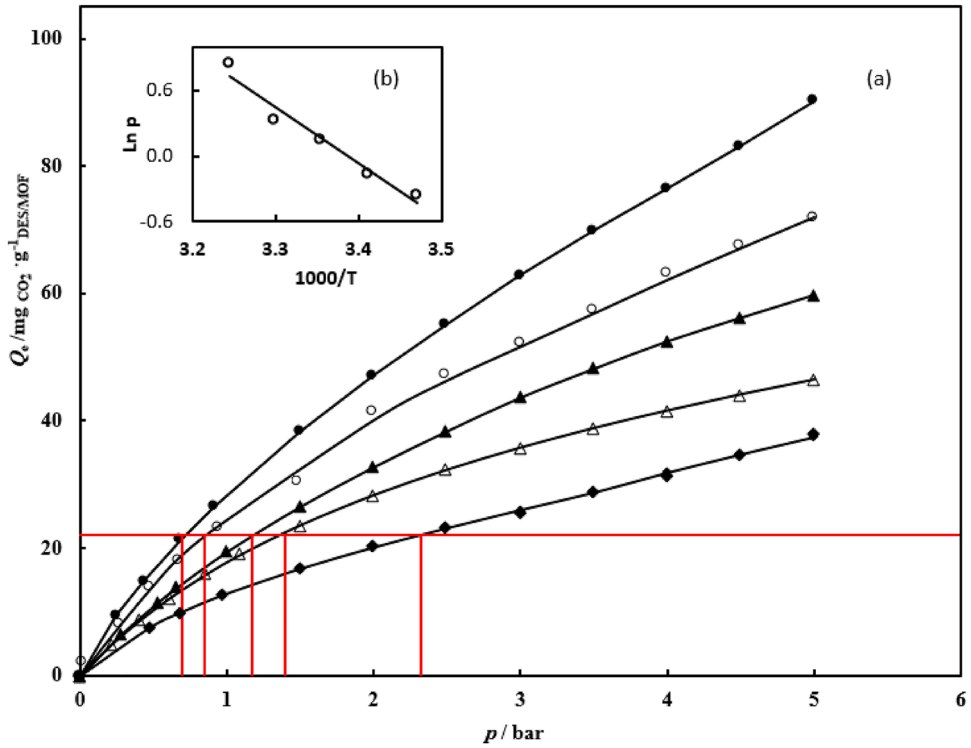

Figure 10. Evaluation isosteric heat of CO_2 adsorption on DES1/NH_2-MIL-53(Al). (**a**) Selection of isosteric pressure at different temperatures: (●) 288.15 K, (○) 293.15 K, (▲) 298.15 (Δ) 303.15 K, (◆) 308.15 K. (**b**) Plot of ln(p) versus 1/T.

DES /NH_2-MIL-53	ΔH/kJ mol^{-1}	
	CO_2	N_2
NH_2-MIL-53(Al)	− 38.99 ± 0.90	− 32.65 ± 0.65
DES1/NH_2-MIL-53(Al)	− 35.50 ± 0.92	− 38.93 ± 0.15
DES2/NH_2-MIL-53(Al)	− 40.78 ± 0.23	− 29.46 ± 0.35
DES3/NH_2-MIL-53(Al)	− 38.52 ± 0.48	− 33.19 ± 0.90

Table 7. The molar enthalpy of absorption for NH_2-MIL-53 and DESs /NH_2-MIL-53.

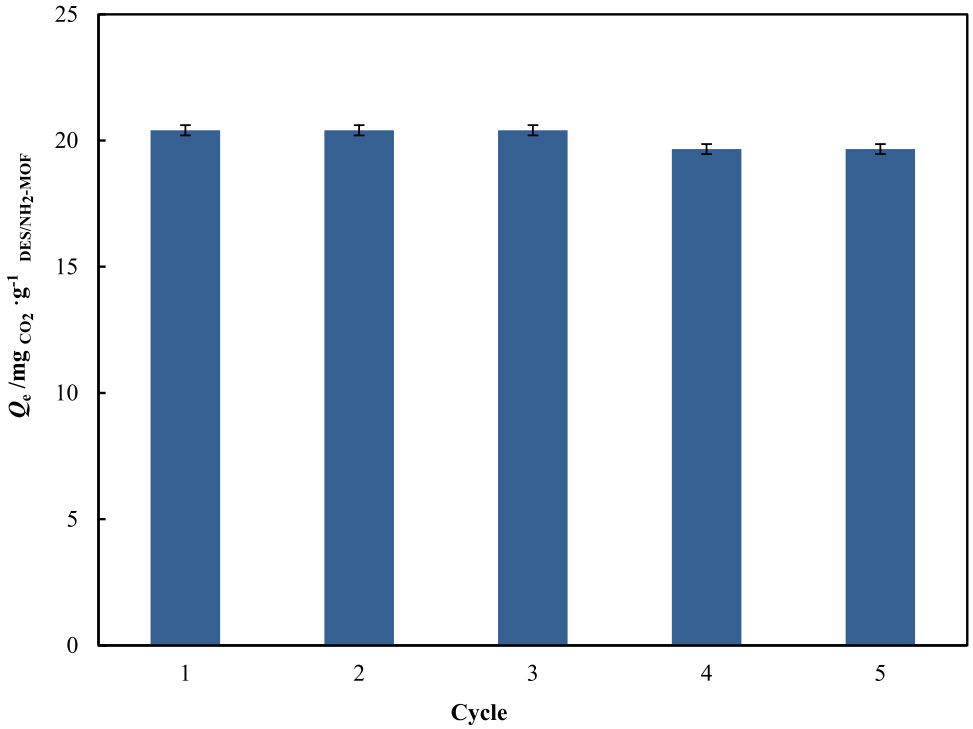

Figure 11. The CO_2 absorption capacity of DES1/NH_2-MIL-53(Al) at $p = 1.000$ bar and $T = 298.15$ K in five adsorption/desorption cycles.

Data availability

The datasets used and/or analyzed during the current study available from the corresponding author on reasonable request.

Received: 28 April 2023; Accepted: 6 August 2023
Published online: 10 August 2023

References

1. Kang, S., Chung, Y. G., Kang, J. H. & Song, H. CO_2 absorption characteristics of amino group functionalized imidazolium-based amino acid ionic liquids. *J. Mol. Liq.* **297**, 111825 (2020).
2. Ma, L., Svec, F., Tan, T. & Lv, Y. Mixed matrix membrane based on cross-linked poly[(ethylene glycol) methacrylate] and metal–organic framework for efficient separation of carbon dioxide and methane. *ACS Appl. Nano Mater.* **1**, 2808–2818 (2018).
3. Krishnan, A. *et al.* Ionic liquids, deep eutectic solvents and liquid polymers as green solvents in carbon capture technologies: A review. *Environ. Chem. Lett.* **18**, 2031–2054 (2020).
4. Anderson, T. R., Hawkins, E. & Jones, P. D. CO_2, the greenhouse effect and global warming: From the pioneering work of Arrhenius and Callendar to today's Earth System Models. *Endeavour* **40**, 178–187 (2016).
5. Pianta, S., Rinscheid, A. & Weber, E. U. Carbon capture and storage in the United States: Perceptions, preferences, and lessons for policy. *Energy Policy* **151**, 112149 (2021).
6. Barzagli, F., Mani, F. & Peruzzini, M. A ^{13}C NMR study of the carbon dioxide absorption and desorption equilibria by aqueous 2-aminoethanol and Nmethylsubstituted 2-aminoethanol. *Energy Environ. Sci.* **2**, 322–330 (2009).
7. Mandal, B. P., Kundu, M. & Bandyopadhyay, S. S. Physical solubility and diffusivity of N_2O and CO_2 into aqueous solutions of (2-amino-2-methyl-1-propanol + 20 monoethanolamine) and (N-methyldiethanolamine + monoethanolamine). *J. Chem. Eng. Data* **50**, 352–358 (2005).
8. Ebner, A. D. & Ritter, J. A. State-of-the-art adsorption and membrane separation processes for carbon dioxide production from carbon dioxide emitting industries. *Sep. Sci. Technol.* **44**, 1273–1421 (2009).
9. Serna-Guerrero, R., Dana, E. & Sayari, A. New insights into the interactions of CO_2 with amine-functionalized silica. *Ind. Eng. Chem. Res.* **47**, 9406–9412 (2008).
10. Wang, Z. & Cohen-Seth, M. Postsynthetic covalent modification of a neutral metal–organic framework. *J. Am. Chem. Soc.* **129**(41), 12368–12369 (2007).
11. Mondal, M. K., Balsora, H. K. & Varshney, P. Progress and trends in CO_2 capture/separation technologies: A review. *Energy* **46**, 431–441 (2012).
12. Keskin, S. & Sholl, D. S. Selecting metal organic frameworks as enabling materials in mixed matrix membranes for high efficiency natural gas purification. *Energy Environ. Sci.* **3**, 343–351 (2010).
13. Mason, J. A. *et al.* Application of a high-throughput analyzer in evaluating solid adsorbents for post-combustion carbon capture via multicomponent adsorption of CO_2, N_2, and H_2O. *J. Am. Chem. Soc.* **137**, 4787–4803 (2015).
14. Zhang, J., Singh, R. & Webley, P. A. Alkali and alkaline-earth cation exchanged chabazite zeolites for adsorption based CO_2 capture. *Microporous Mesoporous Mater.* **111**, 478–487 (2008).
15. Bernal, M. P., Coronas, J., Menendez, M. & Santamaria, J. Separation of CO_2/N_2 mixtures using MFI-type zeolite membranes. *AIChE J.* **50**, 127–135 (2004).
16. Arstad, B., Fjellvag, H., Kongshaug, K. O., Swang, O. & Blom, R. Amine functionalised metal organic frameworks (MOFs) as adsorbents for carbon dioxide. *Adsorption* **14**, 755–762 (2008).

17. Ellen-Dautzenberg, E., Li, G. & Smet-Louis, C. P. M. Aromatic amine-functionalized covalent organic frameworks (COFs) for CO2/N2 separation. *ACS Appl. Mater. Interfaces* **15**(4), 5118–5127 (2023).
18. Ariyanto, T. *et al.* Improving the separation of CO_2/CH_4 using impregnation of deep eutectic solvents on porous Carbon. *ACS Omega* **6**, 19194–19201 (2021).
19. Lin, H. *et al.* Nanoconfined deep eutectic solvent in laminated MXene for efficient CO_2 separation. *Chem. Eng. J.* **405**, 126961 (2021).
20. Sumida, K. *et al.* Carbon dioxide capture in metal-organic frameworks. *J. R. Long Chem. Rev.* **112**, 724–781 (2012).
21. Nugent, P. *et al.* Porous materials with optimal adsorption thermodynamics and kinetics for CO_2 separation. *Nature* **495**, 80–84 (2013).
22. Olajire, A. A. CO_2 capture and separation technologies for end-of-pipe applications a review. *Energy* **35**, 2610–2628 (2010).
23. Yu, C. H., Huang, C. H. & Tan, C. S. A review of CO_2 capture by absorption and adsorption. *Aerosol Air Qual. Res.* **12**, 745–769 (2012).
24. Torralba-Calleja, E., Skinner, J. & Gutiérrez-Tauste, D. CO_2 capture in ionic liquids: A review of solubilities and experimental methods. *J. Chemother.* **2013**, 473584 (2013).
25. Zhang, X. *et al.* Carbon capture with ionic liquids: Overview and progress. *Energy Environ. Sci.* **5**, 6668–6681 (2012).
26. Smith, E. L., Abbott, A. P. & Ryder, K. S. Deep eutectic solvents (DESs) and their applications. *Chem. Rev.* **114**, 11060–11082 (2014).
27. Sánchez-Sánchez, M. *et al.* Synthesis of metal–organic frameworks in water at room temperature: Salts as linker sources. *Green Chem.* **17**, 1500–1509 (2015).
28. Chen, X. Y., Hoang, V. T., Rodrigue, D. & Kaliaguine, S. Optimization of continuous phase in amino-functionalized metal-organic framework (MIL-53) based co-polyimide mixed matrix membranes for CO_2/CH_4 separation. *RSC Adv.* **3**, 24266–24279 (2013).
29. Sarmad, Sh., Nikjoo, D. & Mikkola, J. P. Amine functionalized deep eutectic solvent for CO_2 capture: Measurements and modeling. *J. Mol. Liq.* **309**, 113159 (2020).
30. Sorribas, S., Gorgojo, P., Tellez, C., Coronas, J. & Livingston, A. G. High flux thin film nanocomposite membranes based on metal-organic frameworks for organic solvent nanofiltration. *J. Am. Chem. Soc.* **135**, 15201–15208 (2013).
31. Noorani, N., Mehrdad, A. & Ahadzadeh, I. CO_2 absorption in amino acid-based ionic liquids: Experimental and theoretical studies. *Fluid Phase Equilib.* **547**, 113185 (2021).
32. Noorani, N., Mehrdad, A. & Chakhmaghi, F. Thermodynamic study on carbon dioxide and methane permeability in polyvinyl-chloride/ionic liquid blends. *Chem. Thermodyn.* **145**, 106094 (2020).
33. Noorani, N. & Mehrdad, A. Experimental and theoretical study of CO_2 sorption in biocompatible and biodegradable cholinium-based ionic liquids. *Sep. Purif. Technol.* **254**, 117609 (2021).
34. Noorani, N. & Mehrdad, A. Cholinium-amino acid ionic liquids as biocompatible agents for carbon dioxide absorption. *J. Mol. Liq.* **357**, 119078 (2022).
35. Noorani, N., Mehrdad, A. & Zareidiznab, R. Thermodynamic study on carbon dioxide absorption in vinyl imidazolium–amino acid ionic liquids. *Fluid Phase Equilib.* **557**, 113433 (2022).
36. Redlich, O. & Peterson, D. L. A useful adsorption isotherm. *J. Phys. Chem.* **63**(1024), 1024–1024 (1959).
37. Seoane, B., Téllez, C., Coronas, J. & Staudt, C. NH2-MIL-53(Al) andNH2-MIL-101(Al) insulfur-containing copolyimide mixed matrix membranes for gas separation. *Sep. Purif. Technol.* **111**, 72–81 (2013).
38. Vimont, A. *et al.* Evidence of CO_2 molecule acting as an electron acceptor on a nanoporous metal–organic-framework MIL-53 or $Cr^{3+}(OH)(O_2C–C_6H_4–CO_2)$. *Chem. Commun.* **21**, 3291–3293 (2007).
39. Cheng, X. *et al.* Size- and morphologycontrolled H2-MIL-53(Al) prepared in DMF-water mixed solvents. *Dalton Trans.* **42**, 13698–13705 (2013).
40. Rouquerol, J., Rouquerol, F., Llewellyn, P., Maurin, G. & Sing, K. S. W. *Adsorption by Powders and Porous Solids* 2nd edn. (Academic Press, 2013).
41. Kim, J., Kim, W. Y. & Ahn, W. S. Amine-functionalized MIL-53(Al) for CO_2/N_2 separation: Effect of textural properties. *Fuel* **102**, 574–579 (2012).
42. Ariyanto, T., Prasetyo, I., Mukti, N. F., Cahyono, R. B. & Prasetya, A. Nanoporous carbon based palm kernel shell and Its characteristics of methane and carbon dioxide adsorption. *IOPConf. Ser. Mater. Sci. Eng.* **736**, 022057 (2020).
43. Kenarsari, S. D. *et al.* Review of recent advances in carbon dioxide separation and capture. *RSC Adv.* **3**, 22739–22773 (2013).
44. Mahdipoor, H. R., Halladj, R., Babakhani, E. G., Amjad-Iranagha, S. & Sadeghzadeh Ahari, J. Synthesis, characterization, and CO_2 adsorption properties of metal organic framework Fe-BDC. *RSC Adv.* **11**, 5192–5203 (2021).
45. Builes, S., Sandler, S. I. & Xiong, R. Isosteric heats of gas and liquid adsorption. *Langmuir* **29**, 10416–10422 (2013).
46. Sircar, S., Mohr, R., Ristic, C. & Rao, M. B. Isosteric heat of adsorption: Theory and experiment. *J. Phys. Chem. B* **103**, 6539–6546 (1999).
47. Marathe, R. P., Farooq, S. & Srinivasan, M. P. Modeling gas adsorption and transport in small-pore titanium silicates. *Langmuir* **21**, 4532–4546 (2005).
48. Pourebrahimi, S., Kazemeini, M., Ganji Babakhani, E. & Taheri, A. Removal of the CO_2 from flue gas utilizing hybrid composite adsorbent MIL-53(Al)/GNP metal-organic framework. *Microporous Mesoporous Mater.* **218**, 144–152 (2015).

Acknowledgements

The authors would thank for postdoctoral grant (No: SAD/3938-1400 1225) from university of Tabriz.

Author contributions

N.N.: data duration, writing-original draft preparation, visualization, investigation. A.M.: conceptualization, methodology, validation, writing-reviewing and editing.

Competing interests

The authors declare no competing interests.

Additional information

Correspondence and requests for materials should be addressed to A.M.

Reprints and permissions information is available at www.nature.com/reprints.

Publisher's note Springer Nature remains neutral with regard to jurisdictional claims in published maps and institutional affiliations.